University of Groningen

Structural and functional characterization of a family GH53 β-1,4-galactanase from Bacteroides thetaiotaomicron that facilitates degradation of prebiotic galactooligosaccharides

Böger, Markus; Hekelaar, Johan; van Leeuwen, Sander S; Dijkhuizen, Lubbert; Lammerts van Bueren, Alicia

IMPORTANT NOTE: You are advised to consult the publisher's version (publisher's PDF) if you wish to cite from it. Please check the document version below.

Document Version
Version created as part of publication process; publisher's layout; not normally made publicly available

[Link to publication in University of Groningen/UMCG research database](#)

Structural and functional characterization of a family GH53 β-1,4-galactanase from *Bacteroides thetaiotaomicron* that facilitates degradation of prebiotic galactooligosaccharides

Markus Böger[a,1], Johan Hekelaar[b,1], Sander S. van Leeuwen[a,2], Lubbert Dijkhuizen[a,3], Alicia Lammerts van Bueren[a,*]

[a] Microbial Physiology, Groningen Biomolecular Sciences and Biotechnology Institute (GBB), University of Groningen, Nijenborgh 7, 9747AG Groningen, The Netherlands
[b] Protein Crystallography, Groningen Biomolecular Sciences and Biotechnology Institute (GBB), University of Groningen, Nijenborgh 7, 9747AG Groningen, The Netherlands

ABSTRACT

Galactooligosaccharides (GOS) are prebiotic compounds synthesized from lactose using bacterial enzymes and are known to stimulate growth of beneficial bifidobacteria in the human colon. *Bacteroides thetaiotaomicron* is a prominent human colon commensal bacterial species that hydrolyzes GOS using an extracellular Glycosyl Hydrolase (GH) family GH53 endo-galactanase enzyme (BTGH53), releasing galactose-based products for growth. Here we dissect the molecular basis for GOS activity of this *B. thetaiotaomicron* GH53 endo-galactanase. Elucidation of its X-ray crystal structure revealed that BTGH53 has a relatively open active site cleft which was not observed with the bacterial enzyme from *Bacillus licheniformis* (BLGAL). BTGH53 acted on GOS with degree of polymerization ≤ 3 and therefore more closely resembles activity of fungal GH53 enzymes (e.g. *Aspergillus aculeatus* AAGAL and *Meripileus giganteus* MGGAL). Probiotic lactobacilli that lack galactan utilization systems constitute a group of bacteria with relevance for a healthy (infant) gut. The strains tested were unable to use GOS ≥ DP3. However, they completely consumed GOS in the presence of BTGH53, resulting in clear stimulation of their extent of growth. The extracellular BTGH53 enzyme thus may play an important role in carbohydrate metabolism in complex microbial environments such as the human colon. It also may find application for the development of synergistic synbiotics.

1. Introduction

The human gut is colonized by trillions of bacteria which are collectively called the human gut microbiota. Gut bacteria have tremendous impact on our health and enable humans to degrade most of the food we ingest. In particular bacteria that colonize the human colon are highly specialized in harvesting energy from complex carbohydrates, such as those found in plant material, in complex human glycans and in fungal and bacterial carbohydrates (Ndeh and Gilbert, 2018). To acquire energy from carbohydrates in such extremely competitive environments, bacteria express specific enzymes and transporters to target and degrade these carbohydrate substrates. The presence of particular carbohydrates therefore may largely dictate which bacteria will grow

and persist in the colon. This may allow us to nurture our colonic bacteria by eating a diet full of complex carbohydrates or by ingesting functional carbohydrates as food supplements, such as prebiotics (Fuller and Gibson, 1997).

A prebiotic is generally defined as a "substrate that is selectively utilized by host microorganisms conferring a health benefit" (Gibson et al., 2017). People may ingest prebiotics as a way to promote the growth of healthy gut bacteria in times of intestinal distress, e.g. during antibiotic treatment, infant colic, inflammatory bowel disease or colorectal cancer (Macfarlane et al., 2007). Galactooligosaccharides (GOS) represent one class of prebiotics synthesized from lactose comprising often glucose at the reducing end and a galactose-chain with a degree of polymerization varying from 2 to 6, constituting a mixture of non-

---

digestible carbohydrates based on galactose. GOS are most commonly used in infant formula. Their application in infant formula dates back to the discovery of the stimulatory effect of human milk on colonic bacteria in the last century. Initially, the growth of a prominent infant gut bacterium, *Lactobacillus bifidus* (now known as *Bifidobacterium bifidum),* was linked to milk from breastfeeding mothers (Gauhe et al., 1954; György et al., 1954a,b,c; Norris et al., 1950; Rose et al., 1954). Later it was found to be based on consumption of human milk oligosaccharides, or HMOs (György et al., 1974; György and Rose, 1955). HMOs thus became known as the "bifidus factor" and since then, much research has gone into determining the structures of HMOs (of which there are over 200) and into finding compounds and molecules that mimic the bifidus effect (Polonovski and Montreuil, 1954; Yazawa and Tamura, 1982). In the late 20th century it was shown that enzymatically synthesized GOS are bifidogenic and, similar to HMOs, stimulate the growth of bifidobacteria (Ito et al., 1990; Smart, 1991). HMOs are complex structures and expensive and laborious to synthesize, while GOS are relatively easy to produce at industrial scale and have similar effects on growth of infant colonic microbiota (Bode, 2012; Ito et al., 1993). From the early 2000's onwards the infant nutrition industry started to use GOS to produce an infant formula that mimics the more natural effects of mother's milk (Otieno, 2010).

With the increasing awareness of how strongly the human colonic microbiome is linked to our overall well-being, researchers and food nutritionists alike aim to build up and maintain a healthy and balanced colonic microbiome (Sanders et al., 2010). GOS at least partly fulfill similar roles as HMOs, but further information is required about the specific mechanisms of GOS utilization. Previously we reported that a subset of branched GOS mimic HMOs in the activation of bacterial mucin utilization pathways, which may allow bacterial species to adhere to the mucosal layer and colonize the GI tract (Lammerts et al., 2017). A second mechanism involves direct use of GOS as a nutritional source by colonic bacteria; GOS has been shown to activate galactan/galactose utilization systems in *Bifidobacterium* and *Bacteroides* (Lammerts et al., 2017). One particular enzyme from the galactan utilization system identified as important for GOS utilization by gut bacteria is an extracellular endo-galactanase from the GH53 family as described in the CAZy database (www.cazy.org) (Lombard et al., 2014). Coincidently, several probiotic bifidobacteria and prominent colonic commensal bacterial species that benefit from HMOs for growth also harbor galactan utilization systems and GH53 enzymes (Lammerts et al., 2017; O'Connell Motherway et al., 2013). Recently Thongaram et al. 2017 reported that GOS utilization in lactobacilli, another group of probiotic bacteria with relevance for a healthy (infant) gut, poorly use GOS with higher DP. They are able to grow on lactose, however, involving a dedicated uptake system and an intracellular β-galactosidase. As allochthonous members of the human colon microbiota, they may instead benefit from GOS breakdown products generated by other autochthonous members (Walter, 2008).

As a proven prebiotic, beneficial effects of GOS may also occur through application in synbiotics. In such synergistic synbiotics the prebiotic is supplied as a specific growth substrate for the cognate probiotic bacterium (Kolida and Gibson, 2011). Some studies already have reported the use of GOS in synbiotics, i.e. in combination with a given probiotic strain, but often the synergistic effect of the combination remains to be proven (Krumbeck et al., 2018; Macfarlane et al., 2007).

In earlier work we have identified an extracellular GH53 enzyme from *B. thetaiotaomicron* that is implicated in both pectic galactan and prebiotic GOS utilization and releases galactobiose and galactose as final products of pectic galactan degradation (Lammerts et al., 2017). In the present study, we further characterized this endo-galactanase enzyme in terms of three-dimensional structure and enzymatic activity, in order to further understand its role in GOS degradation. We observed that this enzyme degrades β-1,4-galactan (potato galactan) but not β-1,3-galactan (as found in larch wood arabinogalactan). Its three-

dimensional crystal structure revealed that BTGH53 is similar to fungal GH53s rather than to the bacterial GH53 enzyme characterized from *Bacillus licheniformis* (Le Nours et al., 2003; Ryttersgaard et al., 2002). Specifically, BTGH53 shows a different organization of βα-loops 6, 7 and 8 lacking additional substrate binding sites which is not observed for the *Bc. licheniformis* GH53 enzyme, along with an additional D331 residue in BTGH53 which stabilizes the axial C4 hydroxyl group of galactose in the −1 subsite position. As a result BTGH53 is able to degrade shorter GOS and *p*NP-galactose. Finally, we demonstrate that in the presence of BTGH53 probiotic *Lactobacillus* strains become fully competent to degrade and grow on larger DP GOS. These results show in more detail how GOS are metabolized by GH53 enzymes, and further our understanding of how extracellular CAZymes facilitate growth of beneficial probiotic *Lactobacillus* strains in complex microbial environments.

2. Materials and methods

2.1. Materials

Azo-galactan and galactobiose were purchased from Megazyme (Bray, Ireland). Purified GOS (pGOS derived from Vivinal® GOS with glucose, galactose and lactose largely removed from the commercial product) was provided by FrieslandCampina Domo (Amersfoort, The Netherlands), and P5 GOS by Winclove Probiotics (Amsterdam, the Netherlands). Composition of pGOS has been analyzed and described previously (Lammerts et al., 2017). P5 GOS composition was analyzed as described below. All other compounds were purchased from Sigma (Zwijndrecht, NL). *Bacteroides thetaiotaomicron* VPI-5482 was purchased from DSMZ (DSM 2079, ATCC 29148) (Braunschweig, Germany). *Lactobacillus paracasei* W20, *Lactobacillus casei* W56 and *Lactobacillus salivarius* W57 were a kind gift from Winclove Probiotics (Amsterdam, NL). Crystallization materials were purchased from Molecular Dimensions (Newmarket, UK).

2.2. B. thetaiotaomicron growth experiments

B. thetaiotaomicron growth was carried out as described previously (Lammerts et al, 2017). Briefly, overnight cultures of *B. thetaiotaomicron* were grown at 37 °C in rich medium (Brain Heart infusion broth + 5 mM L-cysteine under anaerobic conditions in an anaerobic jar (Oxoid) with a GasPak (BD). The following day, 1 ml of a 50-fold dilution of a *B. thetaiotaomicron* overnight culture was used to inoculate carbon-limited minimally defined medium with 100 mM KH_2PO_4 (pH 7.2), 15 mM NaCl, 8.5 mM $(NH_4)_2SO_4$, 4 mM L-cysteine, 1.9 mM hematin, 200 mM L-histidine, 100 nM $MgCl_2$, 1.4 nM $FeSO_4\cdot 7H_2O$, 50 mM $CaCl_2$, 1 mg ml^{-1} vitamin K3, 5 ng ml^{-1} vitamin B12 and individual carbon sources (0.5%, wt vol^{-1}). Culture tubes containing 2 ml total volume were prepared in Hungate tubes under anaerobic conditions using Hungate techniques under 100% CO_2 gas (Daniels and Zeikus, 1975). Growth curves were obtained by incubating tubes at 37 °C and taking optical density readings at 600 nm (OD600) at ~1–2 h time intervals over a 4 day period.

2.3. Protein production, crystallization, data collection and structure determination

Production and purification of BTGH53 protein was carried out as described previously (Lammerts et al., 2017). Further purification steps were used to obtain fully purified BTGH53 protein for crystallization experiments. Size exclusion chromatography was performed using Sephadex S75 in buffer containing 20 mM Tris pH 7.5, 150 mM NaCl. Fractions containing the purified protein were pooled and concentrated using an Amicon centricon filter (Millipore) with a 10 KDa MWCO membrane.

Crystallization trials were performed at room temperature using the

sitting-drop vapor diffusion method using commercially available crystallization screens. MRC2 Plates were setup by pipetting 100 nL; 10 mg/ml protein and 100 nL screen condition together using a Mosquito pipetting robot (TTP Labtech Ltd). Crystals were found after a few days up to several weeks at various conditions. Crystals from condition 20% PEG6000, 200 mM NH$_4$Cl, MES pH 6.0 (Wizard Classic 3 & 4 screen, Rigaku) were recognized as most promising single crystals based on size (approximately 185 × 80 × 80 μm) and sharp edges. For determination of the apo protein structure the crystal was transferred in a new drop with a higher PEG6000 concentration of 22% to reach cryo conditions, and directly flash frozen in a stream of nitrogen gas at 110 K. Diffraction data was collected at 110 K using a Microstar rotating anode (Cu) X-ray source (Bruker AXS GmbH) in combination with Helios optics (Incoatec GmbH) and a MAR345dtb detector (Marresearch GmbH). Diffraction images for 130° were recorded with 1° oscillation.

For determination of the galactose bound protein structure, the crystal was transferred to a new drop for 30 s containing a reservoir solution with 50 mM pGOS and flash frozen in liquid nitrogen. The data collection was performed under cryo conditions at the P13 EMBL Beamline (Hamburg, Germany). Diffraction images for 135° were recorded with 0.05° oscillations.

Diffraction images were indexed, integrated, scaled and merged with programs XDS and Aimless (Kabsch, 2010). The structure of the apo BTGH53 protein was determined by the molecular replacement method using Phaser (McCoy et al., 2007) where four homology search models were used. These search models were obtained from the FFAS server blast and the top four score structural homologues (PDB codes: 1FHL; 1HJQ; 4BF7; 1HJS) with 28–31% sequence identity were used to build homology models using the SCWRL modelling method in the mixed atom mode by replacing template residues with serine for unconserved residues between the target and the template except for glycines and alanines (Jaroszewski et al., 2011; Krivov et al., 2009). After Phaser, building the final model was performed with the ARP/wARP program and refinement was done with Refmac5, both from the CCP4 software suite (CP Collaborative, 1994; Winn et al., 2011). For the crystals used in the substrate soak experiment the search coordinates from the apo structure were used.

Crystals belonging to space group *P*2$_1$ contained 2 protein molecules in the asymmetric unit having a solvent content of 39.1%. A summary of the data collection statistics is given in Table 1 and of the refinement statistics in Table 2.

Table 1

Data collection & statistics. Between brackets: Statistics highest resolution shell. *: Department of Biophysical Chemistry.

	Apo BTGH53 (PDB ID 6GP5)	BTGH53 + Galactose (PDB ID 6GPA)
X-ray Facility	University Groningen*	EMBL Hamburg
Wavelength (Å)	1.54	0.98
Space group	*P*2$_1$	*P*2$_1$
mol/A.U	2	2
Solvent content (%)	*39.11%*	*41.24*
Unit-cell parameters		
a, b, c (Å)	47.2, 44.7, 137.6	47.5, 45.6, 138.8
α, β, γ (°)	90.0, 99.4, 90.0	90.0, 99.8, 90.0
Resolution range high (Å)	1.93 (1.98–1.93)	1.79 (1.83–1.79)
Resolution range low (Å)	46.58	46.85
R_{merge}	0.073 (0.324)	0.110 (0.403)
$R_{p.i.m}$	0.053 (0.247)	0.085 (0.328)
Total No. of observations	110,321 (5637)	138,347 (6516)
Total No. of unique reflections	40,545 (2339)	53,053 (2687)
Mean *I*/σ (*I*)	14.06 (3.28)	8.6 (2.8)
Completeness (%)	94.8 (81.1)	96.1 (80.5)
Multiplicity	2.7 (2.4)	2.6 (2.4)

Table 2

Refinement statistics.

	Apo BTGH53 (PDB ID 6GP5)	BTGH53 + galactose (PDB ID 6GPA)
Resolution (Å)	1.93	1.79
R	0.1735	0.170
R_{free}	0.2247	0.220
RMSD from target geometry		
Bond lengths (Å)	0.010	0.0115
Bond angles (°)	1.356	1.4558
Tot. number of atoms	5369	5678
Number of amino acids	625	624
Number of water molecules	430	724
Ramachandran (%)		
Favoured (%)	96	97
Allowed (%)	4	3
Outliers (%)	0	0

2.4. Determination of BTGH53 specific activities

The activity of BTGH53 on the synthetic substrate *p*NP-galactose was determined by measuring the release of 4-nitrophenol at 405 nm. Assays were run using different buffers over a range of pH values: 50 mM sodium acetate pH 5.5, 6.0; 50 mM sodium phosphate pH 6.0, 6.5, 7.0; 20 mM HEPES pH 7.5; 20 mM Tris pH 7.5, 8.0. The molar extinction coefficients used to calculate *p*NP release were 2.31 mM^{-1} cm^{-1} (pH 5.5), 3.66 mM^{-1} cm^{-1} (pH 6.0), 7.38 mM^{-1} cm^{-1} (pH 6.5), 11.39 mM^{-1} cm^{-1} (pH 7.0), 14.22 mM^{-1} cm^{-1} (pH 7.45), 17.26 mM^{-1} cm^{-1} (pH 8.0). Reactions were initiated by the addition of BTGH53 to a final concentration of 5 μM. Reaction rates were plotted against pH producing a bell shaped curve. Optimum pH conditions were found to be 50 mM phosphate buffer pH 7.0 which was used for all subsequent studies.

Enzyme activity was measured with 0.1–15 mM *p*NP-galactose in 50 mM phosphate buffer pH 7.0 using the conditions described above. Reaction rates were monitored continuously at 405 nm for 600 s, the rates were taken as the slope between 300 and 360 s. The data were fitted to the Michaelis-Menten equation in GRAFIT which was used to calculate the K_M and V_{max} values. The V_{max} was adjusted for the enzyme concentration to give the k_{cat} value.

BTGH53 endo-galactanase specific activity was determined using the dyed substrate Azo-galactan according to manufacturer's instructions. A reaction mixture containing 500 μl 2% Azo-galactan in 50 mM phosphate buffer pH 7.0 plus 500 μl of 5 μM BTGH53 in the same buffer was incubated for 10 min at 37 °C. After incubation, the reaction was stopped and the residual high molecular weight polymer was precipitated by the addition of 2.5 ml of cold 100% ethanol. The reaction mixture was centrifuged for 10 min at 2800*g* and the produced low-molecular weight dyed fragments in the supernatant assayed by measuring absorbance at 590 nm. Units of enzyme activity were calculated from absorbance values by using a standard curve supplied by the manufacturer that standardized values of absorbance at 590 nm to amount of reducing sugar ends formed obtained according to the method Nelson/Somogyi (Somogyi, 1952). One unit of activity (GalU/mg) was defined as the amount of enzyme required to release 1 μmol of galactose reducing sugar equivalents from galactan per min.

2.5. Lactobacillus growth curves

Lactobacillus growth curves were measured in microtiter plates as described previously (Boger et al., 2018). In brief, *Lactobacillus* strains were grown in modified MRS medium containing 5 mg ml^{-1} GOS. BTGH53 treated GOS was prepared by incubating 10 mg ml^{-1} GOS with 200 μM BTGH53 in 50 mM sodium phosphate buffer pH 7.0 at 37 °C for 24 h. After digestion, BTGH53 was inactivated by heat

treatment (10 min at 80 °C), any precipitant removed by centrifugation (5 min, 16,000*g*) and samples were filter sterilized using 0.2 µm cellulose acetate filters. After *Lactobacillus* growth, culture supernatants were analyzed for any remaining GOS molecules using high pressure anion exchange chromatography with pulsed amperometric detection (HPAEC-PAD) as previously described (Lammerts et al., 2017).

2.6. Analysis of GOS composition

P5 GOS was analyzed using comparative HPAEC-PAD with known structural components (covering > 99% of the substrate composition) of Vivinal® GOS as reference (van Leeuwen et al., 2016). In brief, P5 GOS was dissolved to 1 mg/ml in 80% (vol vol⁻¹) dimethyl sulfoxide and its composition analyzed on a Dionex DX500 work station equipped with an ED40 pulsed amperometric detection system (HPAEC-PAD). Components were separated on a CarboPac PA-1 column (250 by 5 mm; Dionex) using a system of buffer A = 0.1 M NaOH, buffer B = 0.6 M NaOAc in 0.1 M NaOH, buffer C = deionized water and buffer D = 50 mM NaOAc. Separation was carried out with 10% A, 85% C and 5% D in 25 min to 40% A, 10% C and 50% D, followed by a 35-min gradient to 75% A, 25% B, directly followed by 5 min washing with 100% B and reconditioning with 10% A, 85% B and 5% D for 7 min. Furthermore, P5 GOS was subjected to NMR spectroscopy and known structural-reporter group signals used to evaluate the ^{1}H NMR spectrum of P5 GOS as described by Yin et al. (2017). Briefly, P5 GOS was lyophilized and exchanged twice with 99.9% atom D_2O (Cambridge Isotope Laboratories Ltd, Andover, MA). Then, the sample was dissolved in 650 µl 99.9% atom D_2O, containing 25 ppm acetone as internal standard. The 1D ^{1}H NMR spectra were recorded at a probe temperature of 298 K in a Varian Inova 600 spectrometer (NMR department, University of Groningen, The Netherlands).

2.7. Protein data bank accession codes

Structures of BTGH53 were deposited at PDB with the codes PDB ID 6GP5 (Apo BTGH53) and 6GPA (BTGH53 + Galactose).

3. Results and discussion

3.1. BTGH53 is specific for β-1,4-galactans

We previously reported that BTGH53 is important for degradation of GOS by *B. thetaiotaomicron* and that the enzyme is specific for β-1,4-linked galactans (pectic galactan) and not for the β-1,3-linkage type as found in larch wood arabinogalactans (Lammerts et al., 2017). In the present study BTGH53 was further characterized, both structurally and enzymatically. First, the specific activity of BTGH53 on high molecular weight galactan was determined using the Azo-galactan colorimetric substrate (derived from potato galactan). BTGH53 specific activity with Azo-galactan was as 105.8 ± 0.9 GalU/mg, which is a 10-fold difference lower to the other characterized GH53 enzymes (Ryttersgaard et al., 2004). Previously, we observed that also significant levels of galactose were formed after BTGH53 activity on galactan, similar to what was observed for fungal GH53 enzymes (Lammerts et al., 2017). Therefore exo-activity of BTGH53 was tested with the chromogenic substrate 4-nitrophenyl-β-D-galactopyranoside (*p*NPG). This indeed resulted in yellow color formation due to the release of 4-nitrophenyl, with a pH optimum at pH 7.0 (not shown). BTGH53 displayed Michaelis-Menten kinetics, with a K_M value of 69.7 ± 5.7 µM and a k_{cat} value of 29.6 ± 0.9 s⁻¹ (k_{cat}/K_M value is 425 mM⁻¹ s⁻¹). The moderate turnover rate of BTGH53 on the *p*NPG substrate is similar to that observed for the fungal GH53 enzymes AAGAL and MGGAL (Torpenholt et al., 2011). Hydrolysis decreased above concentrations of 15 mM *p*NPG which may be due to transglycosylation activity of BTGH53, as was also suggested for the fungal GH53 enzymes. BTGH53 was inactive on lactose and galactobiose (mixture of β-D-Gal*p*-(1 → 3)-D-

Gal plus β-D-Gal*p*-(1 → 4)-D-Gal) but able to cleave DP3 GOS (Lammerts et al., 2017). The ability of BTGH53 to hydrolyze galactose from *p*NPG and to cleave DP3 GOS, makes this enzyme more similar to the fungal GH53 endo-galactanases than to the bacterial BLGAL enzyme from *Bc. licheniformis*.

3.2. Structure of BTGH53

In order to gain further insights into the catalytic mechanism of BTGH53, we determined the three-dimensional structure of BTGH53. Native crystals were soaked in 50 mM pGOS in order to get a high resolution structure of BTGH53 in complex with products. We obtained a high resolution data set (1.79 Å) and solved the structure by molecular replacement as described (see Methods). The final model of BTGH53 consisted of amino acid residues 37–350 with two molecules in the asymmetric unit. Each BTGH53 molecule contained one galactose residue in the active site. The high resolution model was refined to give an overall R/Rfree of 0.17/0.22.

The overall fold and architecture of BTGH53 is similar to the other structurally characterized bacterial GH53 enzyme, BLGAL from *Bc. licheniformis* (PDB code 1UR4) (core RMSD 1.48 Å, 32.5% sequence identity) and the closely related fungal AAGAL enzyme of *Aspergillus aculeatus* (PDB code 1FHL, core RMSD 1.49 Å, 29.5% sequence identity) (Fig. 1). The closest structure for the bacterial homologue *Bc. licheniformis* 1UR4 (based on sequence identity) did not work for finding the phases for the BTGH53 structure. An alternative approach to solving the BTGH53 structure was then attempted using the FFAS blast algorithm (http://ffas.sanfordburnham.org/ffas-cgi/cgi/ffas.pl) to obtain the closest structural homologues based on fold and function (Jaroszewski et al., 2011). The top 4 from the FFSA search (PDB codes 4BF7, 1FHL, 1HJS and 1HJQ) were used for finding the phases.

BTGH53 exhibits a (βα)$_8$ TIM barrel fold with the catalytic machinery positioned within the center of the barrel (Fig. 1). The candidate catalytic residues are D132 as acid/base and E180 as nucleophile, based on the position of these catalytic residues within all GH53 enzymes which belong to clan GH-A (CAZy database GH53 https://www.
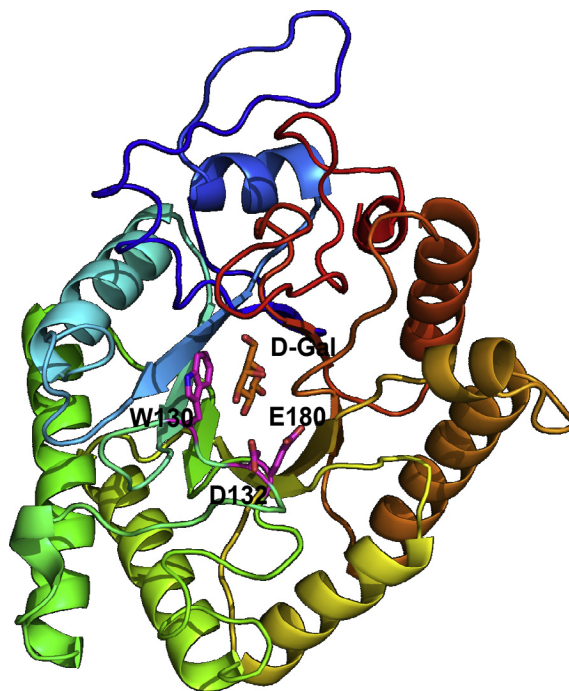

Fig. 1. 3-Dimensional structure of the BTGH53 enzyme in complex with a galactose molecule (orange) showing the organization of a (βα)$_8$-barrel. Residues highlighted in pink are the catalytic residues D132 and E180, and stabilizing residue W130.
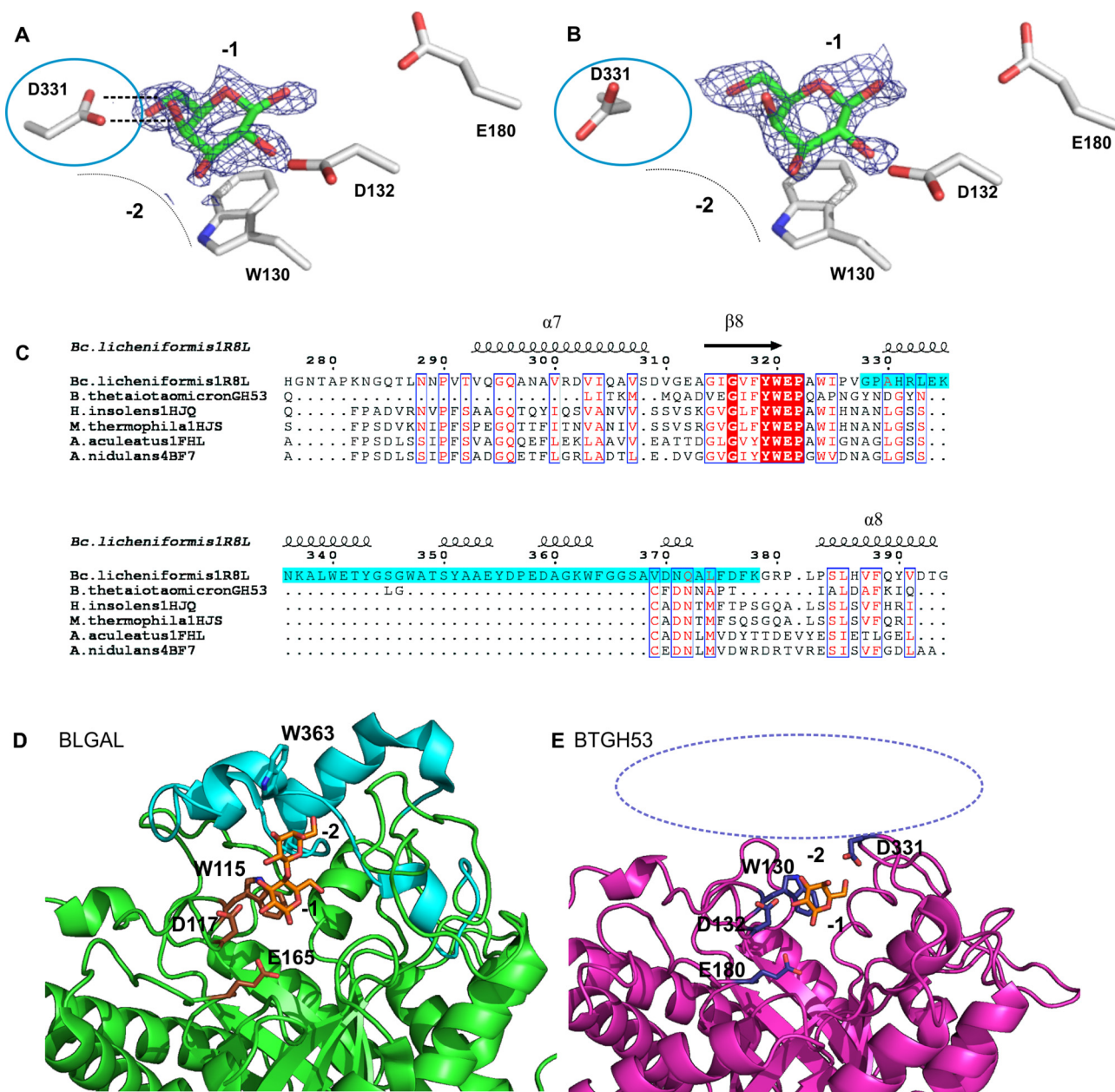
Fig. 2. Structural characteristics original to BTGH53. (A + B) 2*Fo-Fc* omit electron density maps for the original unrefined density, contoured to 1σ, showing the bound galactose. D331 is proposed to play an important role in forming the −2 subsite and we speculate its flexibility, as indicated by the different positions within the individual protein molecules in the asymmetric unit, provides BTGH53 the ability to cleave shorter galactooligosaccharide substrates. (A) protein 1 active site showing hydrogen bonds between D331 and C4 and C6 OH groups, (B) protein 2 active site where D331 is rotated 180° about Cβ with respect to protein A. Amino acids are indicated in grey, galactose molecules are indicated in green, D331 highlighted in blue oval. (C) Amino acid sequence alignment of BTGH53 and BLGAL (PDB code 1R8L) showing the missing loop 8 region in BTGH53; βα-loops numbered according to the structure of BLGAL (Ryttersgaard et al., 2004). Loop 8 is highlighted in light blue in BLGAL (residues 328–378; missing in BTGH53); alignment prepared with ClustalOmega and ESPript (McWilliam et al., 2013; Robert and Gouet, 2014). (D) 3-dimensional organization of the active sites of BLGAL (bound with galactobiose in orange) and (E) BTGH53 (bound with galactose in orange). Catalytic residues of BLGAL (D117 and E165) and corresponding residues D132 and E180 in BTGH53 are shown. Loop 8 region lacking in BTGH53 is highlighted by the (empty) blue circle.

cazypedia.org/index.php/Glycoside_Hydrolase_Family_53; Lombard et al., 2014). These residues align with the catalytic residues D117 and E165 of the GH53 enzyme from *Bc. licheniformis* (PDB code 1UR4).

In one of the protein molecules in the asymmetric unit, the galactose molecule occupying the −1 subsite was stabilized by direct hydrogen bonding with D331 to its C4 and C6 hydroxyl groups, while W130 facilitated stacking interactions with the galactose molecule (Fig. 2A). In the other protein molecule in the asymmetric unit, we observed that D331 is rotated 180° about C_b and does not form hydrogen bonds with galactose occupying the −1 subsite (Fig. 2B). Therefore we speculate

that D331 plays an important role in forming the −2 subsite, where in the presence of galactobiose, the −2 galactose is stabilized by D331, while in its absence, D331 forms hydrogen bonds with galactose in −1. This explains why BTGH53 is active on *p*NP-galactose.

BTGH53 lacks a large loop region within the substrate binding site which is present in BLGAL (Fig. 2C–E). In BLGAL an extended loop 8 from the beta strand at position 8 forms a substrate binding site region with the −3 and −4 substrate binding subsites. The loop 8 region in BLGAL restricts this enzyme from cleaving GOS smaller than DP4 (Ryttersgaard et al., 2004). With the loop 8 region missing in BTGH53,
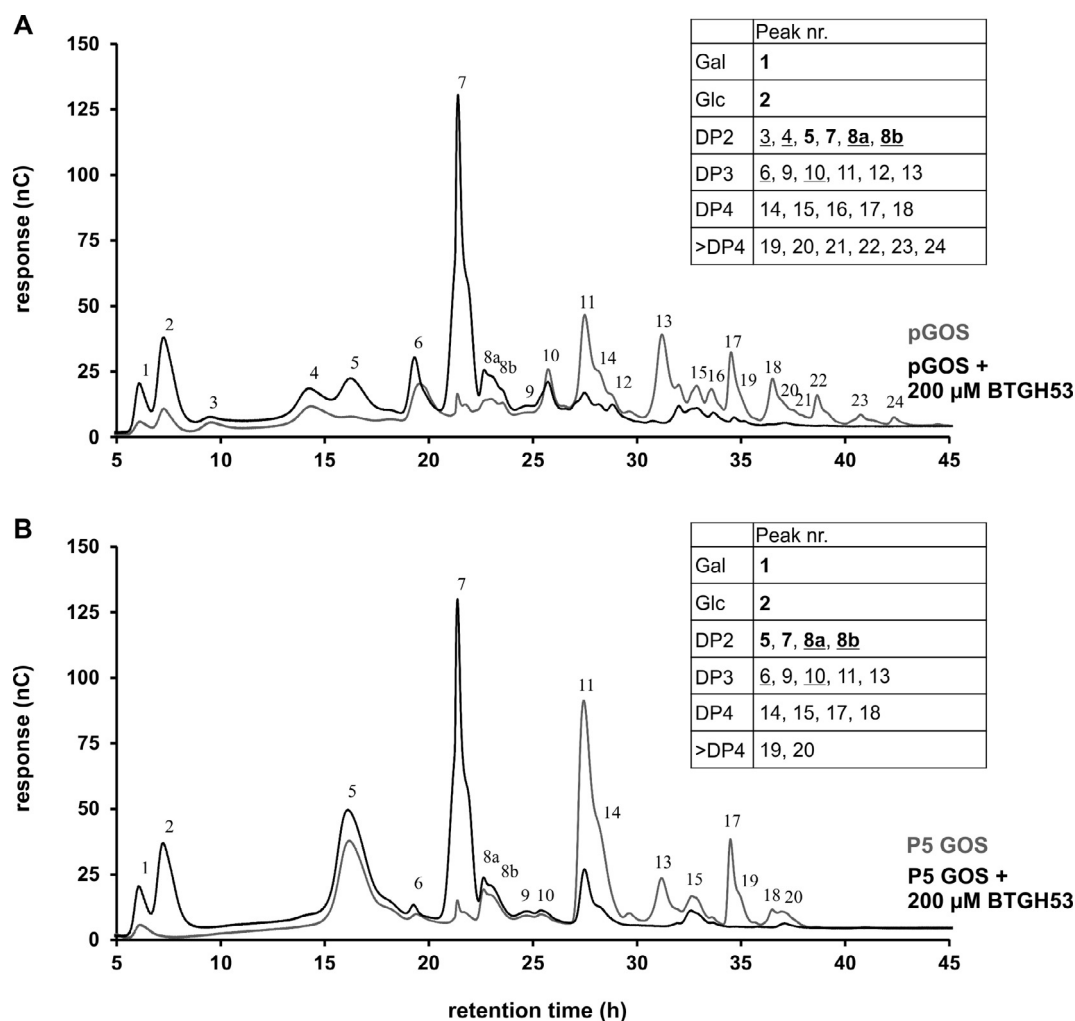
Fig. 3. HPAEC-PAD analysis of 1 mg ml^{-1} pGOS (A) and P5 GOS (B) untreated (grey) and after incubation with BTGH53 (black). Adjacent tables show degree of polymerization of GOS components of corresponding peaks. Peak numbers with increased peak height due to BTGH53 activity are highlighted in bold, underlined peak numbers refer to compounds recalcitrant to BTGH53.
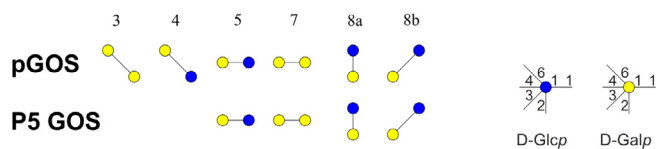

Fig. 4. Structural identity of GOS compounds comprising the DP2 fraction. **3** β-D-Galp-(1 → 6)-D-Gal, **4** β-D-Galp-(1 → 6)-D-Glc (allolactose), **5** β-D-Galp-(1 → 4)-D-Glc (lactose), **7** β-D-Galp-(1 → 4)-D-Gal (galactobiose), **8a** β-D-Galp-(1 → 2)-D-Glc, **8b** β-D-Galp-(1 → 3)-D-Glc. Numbers indicate HPAEC-PAD chromatogram peaks shown in Fig. 3.

the enzyme is able to bind to and act upon smaller substrates, such as galactotriose, producing galactobiose and galactose (Lammerts et al., 2017). This activity makes BTGH53 much more similar to the fungal GH53 enzyme AAGAL (Ryttersgaard et al., 2002).

Due to a truncated loop 8, BTGH53 loop 7 is not linked to loop 8, which is important for active site stability in all other structurally characterized GH53 enzymes (Ryttersgaard et al., 2004). In both AAGAL and BLGAL, loops 7 and 8 are linked via coordination of a calcium ion (BLGAL) or via a disulfide bond (AAGAL). In all fungal GH53 enzymes, the cysteine residues involved in disulfide bond formation are conserved (Le Nours et al., 2003). To correct for this, BTGH53 also has a truncated loop 7 region creating a large gap which is filled by an extended loop 6 region. This loop 6 region forms part of the

BTGH53 active site. This organization has not been observed in any other GH53 structures studied to date. These structural changes in loops 6, 7 and 8 in BTGH53 may have clear effects on its activity and specificity. BTGH53 is active on β-1,4-linked galactan but not on larch arabinogalactan which is primarily β-1,3-galactan (Megazyme Larch Wood arabinogalactan, product code P-ARGAL). The structural changes observed in the substrate binding site of BTGH53 thus may select for only the β-1,4-linkage type and accommodate molecules of shorter DP length as observed previously (Lammerts et al., 2017).

The acid/base D132 residue forms a hydrogen bond with the galactose C2 hydroxyl group, where the E180 carboxyl group can perform nucleophilic attack on C1. Because of the loop 8 truncation in BTGH53, an important W363 residue (Fig. 2D) which forms stacking interactions with the galactose in the BLGAL −2 subsite is missing in the BTGH53 structure which may explain why we did not observe a second galactose molecule in the BTGH53 active site (Fig. 2D + E).

A total of five GH53 structures (http://www.cazy.org/GH53_structure.html) have been solved to date, four from eukaryotic soil fungi and one from a soil bacterium. BTGH53 is the second bacterial GH53 enzyme whose structure has been solved, the first from a bacterium that resides in the human gastrointestinal tract. The particular niche environment where a microbe resides may influence how its enzymes evolve also with respect to substrate specificity. *B. thetaiotaomicron* is resident in the distal gut, and the extracellular BTGH53 may target non-digestible GOS that reach the distal gut. The observed

Table 3

Growth of *Lactobacillus* strains on 5 mg ml^{-1} GOS and GOS pre-incubated with BTGH53. No exponential growth phase was detected for *L. paracasei* W20 on pGOS. OD600 nm values obtained at stationary growth phase are expressed relative to corresponding OD600 nm values of glucose controls set as 1. All values shown are means of n = 3 biological replicates. n.a., not applicable.

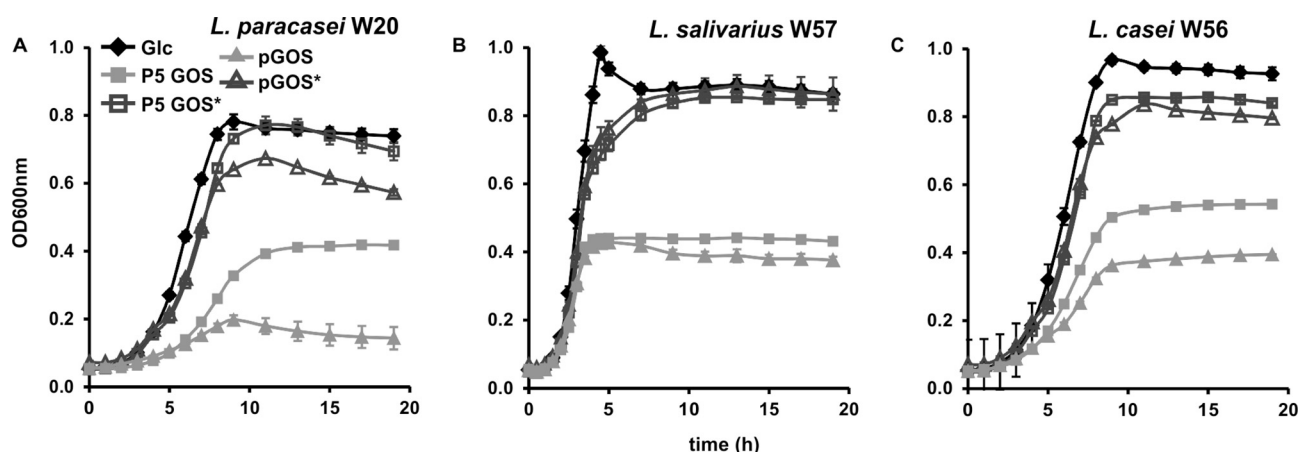|	Relative OD600 at stationary phase (16 h)			
	P5 GOS	P5 GOS + BTGH53	pGOS	pGOS + BTGH53
L. salivarius W57	0.46 ± 0.01	0.97 ± 0.01	0.41 ± 0.02	0.99 ± 0.03
L. paracasei W20	0.47 ± 0.01	0.99 ± 0.02	0.19 ± 0.02	0.86 ± 0
L. casei W56	0.63 ± 0	0.93 ± 0	0.47 ± 0	0.88 ± 0
	Growth rates (h^{-1})			
	P5 GOS	P5 GOS + BTGH53	pGOS	pGOS + BTGH53
L. salivarius W57	0.27 ± 0.01	0.37 ± 0	0.21 ± 0	0.38 ± 0.02
L. paracasei W20	0.07 ± 0	0.18 ± 0	n.a.	0.16 ± 0
L. casei W56	0.10 ± 0	0.20 ± 0	0.07 ± 0	0.2 ± 0

Fig. 5. Anaerobic growth of *L. paracasei* W20 (A), *L. salivarius* W57 (B), *L. casei* W56 (C) with 5 mg ml^{-1} pGOS and P5 GOS, pure and (*) BTGH53 digested. Glucose (5 mg ml^{-1}) served as positive control. In some cases error bars are smaller than symbols and therefore not apparent.

changes to the BTGH53 active site thus may allow *B. thetaiotaomicron* to efficiently degrade galactan compounds of the β-1,4-linkage type down to its smallest constituents. The *B. thetaiotaomicron* galactan utilization system is part of a higher order system that allows degradation of all pectin components with a backbone of β-1,4-galactan, such as rhamnogalacturonans (Ndeh et al., 2017). Only exposure to pectic galactan, and not arabinogalactan of the β-1,3-linkage type (such as larch wood), upregulates the expression of this system and its BTGH53 enzyme. The structural similarity of higher DP GOS to pectic galactan also activates the expression of BTGH53. Therefore the production of the GH53 enzyme is a feature associated with efficient GOS utilization in *B. thetaiotaomicron*.

3.3. Effects of BTGH53 activity on growth of probiotic lactobacilli

Lactobacilli constitute probiotic bacterial strains that very specifically utilize GOS with a degree of polymerization ≤2 (Thongaram et al., 2017). Pure cultures of *Lactobacillus* strains tested hardly consumed prebiotic GOS and thus were unable to grow with GOS as carbon sources. Therefore we subsequently tested whether treatment of GOS with BTGH53 activity actually stimulated growth of probiotic lactobacilli on GOS mixtures.

Two commercial GOS preparations were used, pGOS and P5 GOS. Their composition was analyzed recently using HPAEC-PAD and NMR spectroscopy to elucidate structural identity of nearly all their components (40 and 26, respectively) (van Leeuwen et al., 2014, 2016; Figs. S1 and S2). In brief, in pGOS we identified a total of 40 compounds with different degrees of polymerization (DP) (mostly DP 3–6) and/or

glycosidic linkages (Fig. 3A). Its major component by peak height in the HPAEC-PAD chromatogram was the trisaccharide 4′-galactosyllactose (peak 11, Fig. 3A). Also DP4 compounds, linear and branched, constituted a major fraction of pGOS (28% of total GOS mixture). Comparative HPAEC-PAD analysis of pGOS and P5 GOS, followed by NMR analysis of P5 GOS, also allowed elucidation of the P5 GOS structures (Figs. S1 and S2). All 26 GOS structures found in P5 GOS were also found in pGOS, but in clearly different ratios (Fig. 3B). The two major components were DP3 4′-galactosyllactose (as in pGOS) and the corresponding elongated product DP4 β-D-Gal*p*-(1 → 4)-β-D-Gal*p*-(1 → 4)-β-D-Gal*p*-(1 → 4)-D-Glc (Fig. 3B). Together these two linear DP3 and DP4 components constituted up to 44% of total GOS composition in P5 GOS (24% in pGOS). P5 GOS and pGOS differed at the level of branched DP3 and DP4 components. Compounds eluting as peak 10 and 16 were nearly absent in P5 GOS (7% and 5% in pGOS) (Figs. 3B and S1). Also compounds with DP5 and larger were reduced in P5 GOS (5%) in comparison to pGOS (10%). Interestingly, two compounds from the DP2 pool clearly found in pGOS were absent in P5 GOS, allolactose β-D-Gal*p*-(1 → 6)-D-Glc and β-D-Gal*p*-(1 → 6)-D-Gal (Fig. 4). Finally, lactose was still present in P5 GOS (13%) which was removed in pGOS.

Growth of probiotic lactobacilli with pGOS and P5 GOS yielded OD 600 nm values at stationary phase between 19 and 63% of positive controls (with glucose) (Table 3). Final OD values for *L. paracasei* W20 and *L. casei* W56 were clearly lower for pGOS than for P5 GOS (Fig. 5). In contrast, *L. salivarius* W57 reached similar OD values with both GOS preparations (0.53 with P5 GOS and 0.49 with pGOS). The results reflect specific GOS utilization preferences of these lactobacilli. HPAEC-PAD analysis of the bacterial culture supernatants at stationary phase
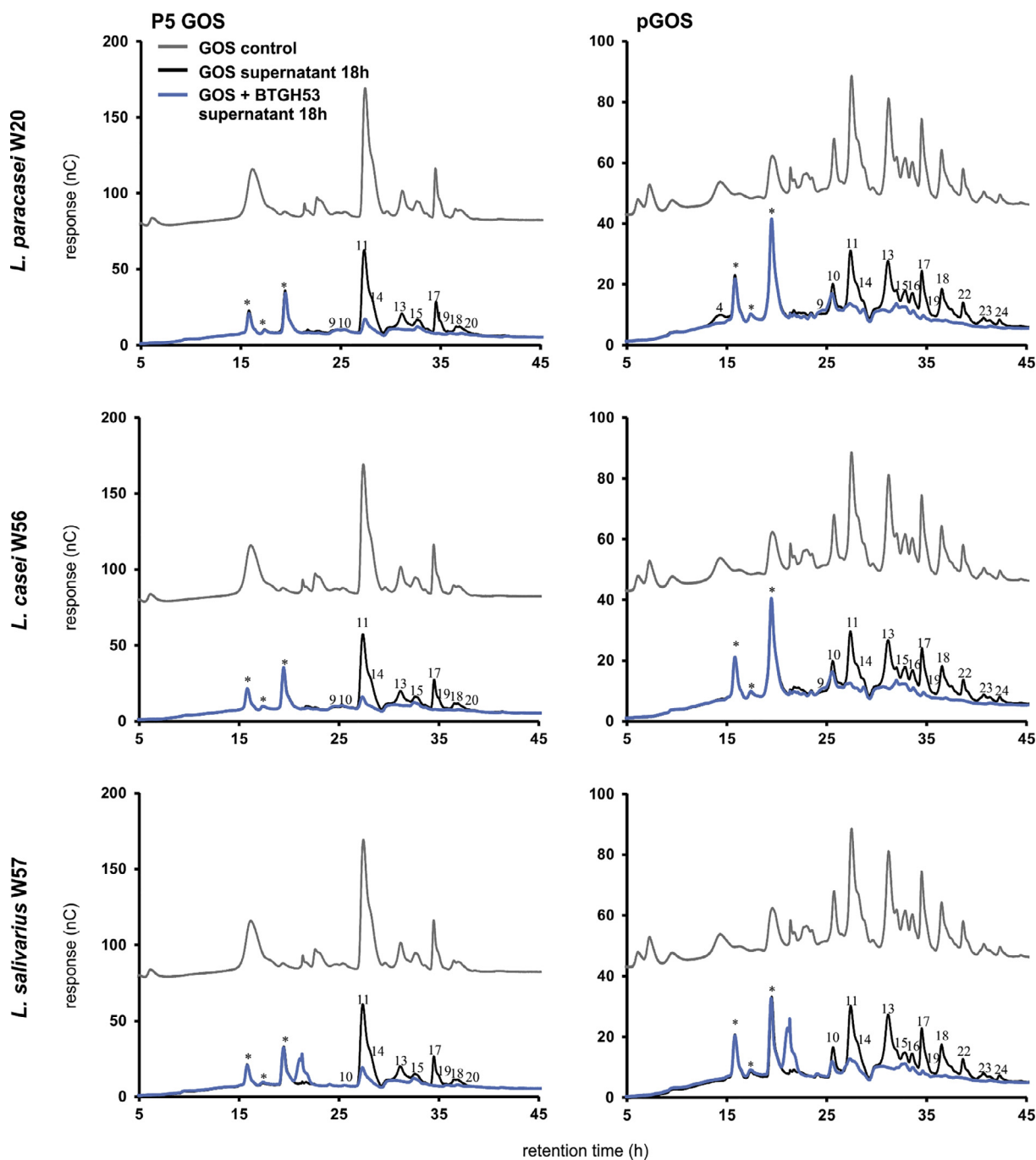
Fig. 6. Utilization of GOS components by probiotic *Lactobacillus* strains analyzed by HPAEC-PAD. Profiles of pGOS and P5 GOS shown in grey (control). Composition of the two GOS preparations in bacterial culture supernatants harvested at stationary growth phase (s. Fig. 5) are shown in black (untreated GOS) and blue (BTGH53 treated GOS). Any GOS components not utilized by probiotic strains in untreated GOS are numbered according to Fig. 3. Peaks arising from medium (mMRS) components are indicated with *.

showed that these lactobacilli differ most clearly in utilization of the various DP2-DP3 GOS. *L. salivarius* W57 consumed any DP2 GOS (peaks 3–8, Fig. 6) present in both GOS and additionally the DP3 GOS component β-D-Gal*p*-(1 → 2)-[β-D-Gal*p*-(1 → 4)-]D-Glc (peak 9, Fig. 6). *L. casei* W56 specifically utilized the DP2 components and *L. paracasei* W20 any DP2 component, but not allolactose (Fig. 6). Similar to *L. paracasei* W20, (Thongaram et al., 2017) recently identified *L. paracasei* LCV-1 as strong utilizer of lactose and a GOS substrate comprising 59% DP2 GOS.

When incubating the two commercial GOS with BTGH53, composition shifted from DP3-DP4 size dominating in untreated GOS to DP2

components in BTGH53 treated GOS. Galactobiose (peak 7, Fig. 3) became the dominating component released to similar levels by BTGH53 treatment. In BTGH53 treated pGOS also the DP2 components β-D-Gal*p*-(1 → 2)-D-Glc, β-D-Gal*p*-(1 → 3)-D-Glc (peaks 8a and 8b, see Figs. 3 and 4) increased, but they remained nearly the same in BTGH53 treated P5 GOS. Besides galactobiose, lactose was the second major component in BTGH53 treated P5 GOS, whereas in BTGH53 treated pGOS the peak heights of lactose and other DP2 components were more equally distributed. Analysis of pGOS products after BTGH53 treatment showed that it was inactive on DP3 branched GOS, the linear DP3 component 6'-galactosyllactose and the DP2 units β-D-Gal*p*-(1 → 2)-D-

Glc, β-D-Gal*p*-(1 → 3)-D-Glc, β-D-Gal*p*-(1 → 6)-D-Gal, β-D-Gal*p*-(1 → 6)-D-Glc. Similar observations were made with P5 GOS. The β-D-Gal*p*-(1 → 6)-D-Gal, β-D-Gal*p*-(1 → 6)-D-Glc compounds were absent in P5 GOS. They also were not found in the chromatogram of BTGH53 treated P5 GOS, thus also not liberated by enzymatic activity with GOS of higher DP. With both GOS samples BTGH53 treatment caused a significant increase in the DP2 compounds β-D-Gal*p*-(1 → 2)-D-Glc, β-D-Gal*p*-(1 → 3)-D-Glc, β-D-Gal*p*-(1 → 4)-D-Gal and β-D-Gal*p*-(1 → 4)-D-Glc (Figs. 3 and 4). This DP2 fraction may specifically stimulate growth of probiotic lactobacilli.

All three lactobacilli clearly benefited from the BTGH53 treatment of the GOS substrates and reached OD values at stationary phase close to positive controls (glucose) (Fig. 5, Table 3). BTGH53 hydrolysis products of P5 GOS stimulated the extent of growth of *L. paracasei* W20 better than the ones obtained from pGOS. BTGH53 treated GOS also resulted in reduced lag phases of growth for *L. paracasei* W20 and *L. casei* W56 (Fig. 5).

HPAEC-PAD analysis demonstrated that lactobacilli consumed a broader range of prebiotic GOS molecules in BTGH53 treated samples than in untreated ones. *L. salivarius* W57 consumed the broadest range of GOS by utilizing any component besides the branched trisaccharides β-D-Gal*p*-(1 → 2)-[β-D-Gal*p*-(1 → 6)-]-D-Glc and β-D-Gal*p*-(1 → 3)-[β-D-Gal*p*-(1 → 4)-]-D-Glc (peak 10, Fig. 6). These two components were also not used by *L. casei* W56 and *L. paracasei* W20 and in addition these two strains didn't consume β-D-Gal*p*-(1 → 2)-[β-D-Gal*p*-(1 → 4)-]-D-Glc (peak 9, Fig. 6) which was also observed with untreated samples. These remaining compounds weren't cleaved by BTGH53 in enzymatic digestions of GOS mixtures (Fig. 3). Overall, pre-treating GOS mixtures with BTGH53 enabled the strains to benefit from a much broader range of GOS molecules with higher DP (Fig. 6).

4. Conclusions

In this paper we have characterized the *B. thetaiotaomicron* BTGH53 β-1,4-galactanase in structural and functional detail. The data shows that BTGH53 activity on prebiotic GOS mixtures results in an increase of DP2 GOS with clear stimulatory effects on growth of lactobacilli. *B. thetaiotaomicron* is a dominant inhabitant of the human colon and probiotic lactobacilli are known to be present in the same compartment (Alander et al., 1999; Saremdamerdji et al., 1995), with potential cross-feeding effects *in vivo*. Similar stimulatory effects may be exerted by extracellular GH53 enzymes from other colon bacteria, but this also depends on their GOS product spectra. The *Bifidobacterium breve galA* gene for instance encodes an extracellular GH53 enzyme (O'Connell Motherway et al., 2013). GalA is an endo-acting galactanase that releases galactotriose as major product instead of galactobiose. Our study shows that lactobacilli are very specific for DP2 GOS utilization and thus will not benefit from products of GalA activity.

Second, our results show that addition of BTGH53 to preparations of probiotic lactobacilli and prebiotic GOS mixtures provides a synbiotic combination: GOS DP2 products released by BTGH53 from longer GOS DP specifically can be utilized for growth by lactobacilli. Such synbiotic combinations may be prepared either by adding (purified) carbohydrate-active enzymes or by pairing probiotic bacteria that (mutually) benefit from each other by producing complementary enzymes on a particular prebiotic substrate.

Declaration of interests

The authors declare that they have no known competing financial interests or personal relationships that could have appeared to influence the work reported in this paper.

Acknowledgements

Appendix A. Supplementary data

References

Alander, M., Satokari, R., Korpela, R., Saxelin, M., Vilpponen-Salmela, T., Mattila-Sandholm, T., von Wright, A., 1999. Persistence of colonization of human colonic mucosa by a probiotic strain, *Lactobacillus rhamnosus* GG, after oral consumption. Appl. Environ. Microbiol. 65, 351–354.

Bode, L., 2012. Human milk oligosaccharides: every baby needs a sugar mama. Glycobiology 22, 1147–1162.

Boger, M.C.L., Lammerts van Bueren, A., Dijkhuizen, L., 2018. Cross-feeding among probiotic bacterial strains on prebiotic inulin involves the extracellular exo-inulinase of *Lactobacillus paracasei* strain W20. Appl. Environ. Microbiol. 84.

CP Collaborative, 1994. The CCP4 suite: programs for protein crystallography. Acta Crystallogr. Sect. D: Biol. Crystallogr. 50, 760–763.

Daniels, L., Zeikus, J.G., 1975. Improved culture flask for obligate anaerobes. Appl. Microbiol. 29, 710–711.

Fuller, R., Gibson, G.R., 1997. Modification of the intestinal microflora using probiotics and prebiotics. Scand. J. Gastroenterol. 32, 28–31.

Gauhe, A., György, P., Hoover, J.R.E., Kuhn, R., Rose, C.S., Ruelius, H.W., Zilliken, F., 1954. Bifidus factor. IV. Preparations obtained from human milk. Arch. Biochem. Biophys. 48, 214–224.

Gibson, G.R., Hutkins, R., Sanders, M.E., Prescott, S.L., Reimer, R.A., Salminen, S.J., Scott, K., Stanton, C., Swanson, K.S., Cani, P.D., Verbeke, K., Reid, G., 2017. The international scientific association for probiotics and prebiotics (ISAPP) consensus statement on the definition and scope of prebiotics. Nat. Rev. Gastroenterol. Hepatol. 14, 491–502.

György, P., Hoover, J.R.E., Kuhn, R., Rose, C.S., 1954a. Bifidus factor. III. The rate of dialysis. Arch. Biochem. Biophys. 48, 209–213.

György, P., Kuhn, R., Rose, C.S., Zilliken, F., 1954b. Bifidus factor. II. Its occurrence in milk from different species and in other natural products. Arch. Biochem. Biophys. 48, 202–208.

György, P., Norris, R.F., Rose, C.S., 1954c. Bifidus factor. I. A variant of *Lactobacillus bifidus* requiring a special growth factor. Arch. Biochem. Biophys. 48, 193–201.

György, P., Rose, C.S., 1955. Further observations on the metabolic requirements of *Lactobacillus bifidus* var. pennsylvanicus. J. Bacteriol. 69, 483–490.

György, P., Jeanloz, R.W., Nicolai, H., Zilliken, F., 1974. Undialyzable growth factors for *Lactobacillus bifidus* var. pennsylvanicus. Protective effect of sialic acid bound to glycoproteins and oligosaccharides against bacterial degradation. Eur. J. Biochem. 43, 29–33.

Ito, M., Deguchi, Y., Miyamori, A., Matsumoto, K., Kikuchi, H., Matsumoto, K., Kobayashi, Y., Yajima, T., Kan, T., 1990. Effects of administration of galactooligosaccharides on the human faecal microflora, stool weight and abdominal sensation. Microb. Ecol. Health Dis. 3, 285–292.

Ito, M., Deguchi, Y., Matsumoto, K., Kimura, M., Onodera, N., Yajima, T., 1993. Influence of galactooligosaccharides on the human fecal microflora. J. Nutr. Sci. Vitaminol. 39, 635–640.

Jaroszewski, L., Li, Z., Cai, X., Weber, C., Godzik, A., 2011. FFAS server: novel features and applications. Nucl. Acids Res. 39, W38–W44.

Kabsch, W., 2010. XDS. Acta Crystallogr. Sect. D: Biol. Crystallogra. 66, 125–132.

Kolida, S., Gibson, G.R., 2011. Synbiotics in health and disease. Annu. Rev. Food Sci. Technol. 2, 373–393.

Krivov, G.G., Shapovalov, M.V., Dunbrack Jr., R.L., 2009. Improved prediction of protein side-chain conformations with SCWRL4. Proteins 77, 778–795.

Krumbeck, J.A., Walter, J., Hutkins, R.W., 2018. Synbiotics for improved human health: recent developments, challenges, and opportunities. Annu. Rev. Food Sci. Technol. 9, 451–479.

Lammerts, V.B., Mulder, M., Leeuwen, S.V., Dijkhuizen, L., 2017. Prebiotic galactooligosaccharides activate mucin and pectic galactan utilization pathways in the human gut symbiont *Bacteroides thetaiotaomicron*. Sci. Rep. 7 40478 40478.

Le Nours, J., Ryttersgaard, C., Lo Leggio, L., Ostergaard, P.R., Borchert, T.V., Christensen, L.L.H., Larsen, S., 2003. Structure of two fungal beta-1,4-galactanases: searching for the basis for temperature and pH optimum. Protein Sci. 12, 1195–1204.

Lombard, V., Ramulu, H.G., Drula, E., Coutinho, P.M., Henrissat, B., 2014. The carbohydrate-active enzymes database (CAZy) in 2013. Nucl. Acids Res. 42, D490–D495.

Macfarlane, G.T., Steed, H., Macfarlane, S., 2007. Bacterial metabolism and health-related effects of galacto-oligosaccharides and other prebiotics. J. Appl. Microbiol. 104, 305–344.

McCoy, A.J., Grosse-Kunstleve, R., Adams, P.D., Winn, M.D., Storoni, L.C., Read, R.J.,

2007. Phaser crystallographic software. J. Appl. Crystallogr. 40, 658–674.

McWilliam, H., Li, W., Uludag, M., Squizzato, S., Park, Y.M., Buso, N., Cowley, A.P., Lopez, R., 2013. Analysis tool web services from the EMBL-EBI. Nucl. Acids Res. 41, W597–W600.

Ndeh, D., Gilbert, H.J., 2018. Biochemistry of complex glycan depolymerisation by the human gut microbiota. FEMS Microbiol. Rev. 42, 146–164.

Ndeh, D., Rogowski, A., Cartmell, A., Luis, A.S., Baslé, A., Gray, J., Venditto, I., Briggs, J., Zhang, X., Labourel, A., Terrapon, N., Buffetto, F., Nepogodiev, S., Xiao, Y., Field, R.A., Zhu, Y., O'Neill, M.A., Urbanowicz, B.R., York, W.S., Davies, G.J., Abbott, D.W., Ralet, M., Martens, E.C., Henrissat, B., Gilbert, H.J., 2017. Complex pectin metabolism by gut bacteria reveals novel catalytic functions. Nature 544, 65–70.

Norris, R.F., Flanders, T., Tomarelli, R.M., György, P., 1950. The isolation and cultivation of Lactobacillus bifidus: a comparison of branched and unbranched strains.

O'Connell Motherway, M., Kinsella, M., Fitzgerald, G.F., van Sinderen, D., 2013. Transcriptional and functional characterization of genetic elements involved in galacto-oligosaccharide utilization by *Bifidobacterium breve* UCC2003. Microb. Biotechnol. 6, 67–79.

Otieno, D.O., 2010. Synthesis of β-galactooligosaccharides from lactose using microbial β-galactosidases. Compr. Rev. Food Sci. Food Saf. 9, 471–482.

Polonovski, M., Montreuil, J., 1954. Chromatographic study of the polyosides of human milk. C. R. Hebd. Seances Acad. Sci. 238, 2263–2264.

Robert, X., Gouet, P., 2014. Deciphering key features in protein structures with the new ENDscript server. Nucl. Acids Res. 42, W320–W324.

Rose, C.S., Kuhn, R., Zilliken, F., György, P., 1954. Bifidus factor. V. The activity of a- and b-methyl-N-acetyl-ᴅ-glucosaminides. Arch. Biochem. Biophys. 49, 123–129.

Ryttersgaard, C., Le Nours, J., Lo Leggio, L., Jorgensen, C.T., Christensen, L.L.H., Bjornvad, M., Larsen, S., 2004. The structure of endo-beta-1,4-galactanase from *Bacillus licheniformis* in complex with two oligosaccharide products. J. Mol. Biol. 341, 107–117.

Ryttersgaard, C., Lo Leggio, L., Coutinho, P.M., Henrissat, B., Larsen, S., 2002. *Aspergillus aculeatus* beta- 1,4-galactanase: substrate recognition and relations to other glycoside hydrolases in clan GH-A. Biochemistry (N.Y.) 41, 15135–15143.

Sanders, M.E., Akkermans, L.M.A., Haller, D., Hammerman, C., Heimbach, J.T.,

Hörmannsperger, G., Huys, G., 2010. Safety assessment of probiotics for human use. Gut Microbes 1, 164–185.

Saremdamerdji, L., Sarem, F., Marchal, L., Nicolas, J., 1995. In vitro colonization ability of human colon mucosa by exogenous *Lactobacillus* strains. FEMS Microbiol. Lett. 131, 133–137.

Smart, J., 1991. Transferase reactions of the beta-galactosidase from *Streptococcus thermophilus*. Appl. Microbiol. Biotechnol. 34, 495–501.

Somogyi, M., 1952. Notes on sugar determination. J. Biol. Chem. 195, 19–23.

Thongaram, T., Hoeflinger, J.L., Chow, J., Miller, M.J., 2017. Prebiotic galactooligosaccharide metabolism by probiotic lactobacilli and bifidobacteria. J. Agric. Food Chem. 65, 4184–4192.

Torpenholt, S., Le Nours, J., Christensen, U., Jahn, M., Withers, S., Østergaard, P.R., Borchert, T.V., Poulsen, J., Lo Leggio, L., 2011. Activity of three β-1,4-galactanases on small chromogenic substrates. Carbohydr. Res. 346, 2028–2033.

van Leeuwen, S.S., Kuipers, B.J.H., Dijkhuizen, L., Kamerling, J.P., 2014. ¹H NMR analysis of the lactose/β-galactosidase-derived galacto-oligosaccharide components of Vivinal® GOS up to DP5. Carbohydr. Res. 400, 59–73.

van Leeuwen, S.S., Kuipers, B.J.H., Dijkhuizen, L., Kamerling, J.P., 2016. Comparative structural characterization of 7 commercial galacto-oligosaccharide (GOS) products. Carbohydr. Res. 425, 48–58.

Walter, J., 2008. Ecological role of lactobacilli in the gastrointestinal tract: implications for fundamental and biomedical research. Appl. Environ. Microbiol. 74, 4985–4996.

Winn, M.D., Ballard, C.C., Cowtan, K.D., Dodson, E.J., Emsley, P., Evans, P.R., Keegan, R.M., Krissinel, E.B., Leslie, A.G.W., McCoy, A., McNicholas, S.J., Murshudov, G.N., Pannu, N.S., Potterton, E.A., Powell, H.R., Read, R.J., Vagin, A., Wilson, K.S., 2011. Overview of the CCP4 suite and current developments. Acta Crystallogr. Sect. D: Biol. Crystallogr. 67, 235–242.

Yazawa, K., Tamura, Z., 1982. Search for sugar sources for selective increase of bifidobacteria. Bifidobacteria Microflora 1, 39–44.

Yin, H., Bultema, J.B., Dijkhuizen, L., van Leeuwen, S.S., 2017. Reaction kinetics and galactooligosaccharide product profiles of the beta-galactosidases from *Bacillus circulans*, *Kluyveromyces lactis* and *Aspergillus oryzae*. Food Chem. 225, 230–238.